Int J Fract (2012) 175:65–71
DOI 10.1007/s10704-012-9696-0

LETTERS IN FRACTURE AND MICROMECHANICS

A RESIDUAL STRESS INTENSITY FACTOR SOLUTION FOR KNOOP INDENTATION CRACKS

Tanja Lube [1)], Theo Fett [2)], Stefan Fünfschilling [2,*)], Michael J. Hoffmann [2)], Rainer Oberacker [2)]

[1)] *Institut für Struktur- und Funktionskeramik, Montanuniversitaet Leoben, Franz-Josef-Straße 18, A-8700 Leoben, Austria*
email: tanja.lube@unileoben.ac.at
[2)] *Institut für Angewandte Materialien - Keramik im Maschinenbau, Universität Karlsruhe, Haid- und- Neu-Straße 7, D-76131 Karlsruhe, Germany*
[*)] *now at: sia Abrasives, Mühlewiesenstrasse 20, CH-8501 Frauenfeld*

Abstract. The residual stress intensity factors at the surface and at the deepest point of the semi-elliptical Knoop indentation crack is determined from the stresses in the damaged zone below the indenter. For this purpose, the weight function approach by Cruse and Besuner was used and wide-range expressions of the geometric function are given. The solution is then applied to a commercial silicon nitride for which all relevant geometrical data are available.

Keywords: Knoop indentation crack, silicon nitride, stress intensity factor

A RESIDUAL STRESS INTENSITY FACTOR SOLUTION FOR KNOOP INDENTATION CRACKS

Tanja Lube [1)], Theo Fett [2)], Stefan Fünfschilling [2,*)], Michael J. Hoffmann [2)], Rainer Oberacker [2)]

1) Institut für Struktur- und Funktionskeramik, Montanuniversitaet Leoben, Franz-Josef-Straße 18, A-8700 Leoben, Austria
Phone: +43(0)3842/402-4111
Fax: +43(0)3842/402-4102
email: tanja.lube@unileoben.ac.at

2) Institut für Angewandte Materialien - Keramik im Maschinenbau, Universität Karlsruhe, Haid- und- Neu-Straße 7, D-76131 Karlsruhe, Germany
**) now at: sia Abrasives, Mühlewiesenstrasse 20, CH-8501 Frauenfeld*

Abstract. The residual stress intensity factors at the surface and at the deepest point of the semi-elliptical Knoop indentation crack is determined from the stresses in the damaged zone below the indenter. For this purpose, the weight function approach by Cruse and Besuner was used and wide-range expressions of the geometric function are given. The solution is then applied to a commercial silicon nitride for which all relevant geometrical data are available.

Keywords: Knoop indentation crack, silicon nitride, stress intensity factor

Introduction

Knoop indentation tests carried out on brittle materials are accompanied by the generation of a half-elliptical surface crack below the indenter which fully develops during unloading by the action of the residual stresses. For the fracture mechanics analysis of such cracks the stress intensity factor caused by the residual stress field is necessary. The simplest approach is to approximate the residual crack opening stresses as a point load at the centre of the indentation (Lawn et al. 1980). This approach yields accurate results for cracks produced by Vickers indenters and other near-axisymmetric indenters, over a wide range of materials and indentation loads. It also provides a reasonable approximation for certain characteristics (e.g. load-crack length relation) of the surface traces of cracks produced by Knoop indenters in the limit of high indentation loads. However, the elongated deformation zone produced by the Knoop indenter results in a crack geometry that departs significantly from the semicircular shape predicted from the point-load solution.
As visible from experiments, a Knoop indentation crack can be very well described by a semi-ellipse. The local stress intensity factor for such cracks has been computed by Keer et al. (1986). Unfortunately, there is no full solution available in literature covering the four main parameters as crack length at the surface ($2c$), crack aspect ratio (a/c), and length ($2b_1$) and aspect ratio (b_1/b_2) of the residual stress region (Fig. 1a). The complicated stress distribution calls for

application of stress intensity factor computation according to the weight function procedure by Cruse and Besuner (1975). By this method, successfully used in fracture mechanics of metals (see e.g. Görner et al. 1983, Caspers et al. 1990, Mahmoud 1990), the weight function can be simply extended to two-dimensional cracks and enables any complicated normal stress distribution to be evaluated.

2. Stress intensity factors for semi-elliptical cracks

A simple fracture mechanics tool to compute the shape of semi-elliptical surface cracks is the computation of the stress intensity factors, K, according to Cruse and Besuner (1975). The stress intensity factors are computed from the actual stress distribution σ and the change of the virtual crack opening displacement field v_r under the reference stress, resulting in the reference stress intensity factor, K_{Ir}, for the considered virtual increase of the crack

$$K = \frac{E'}{K_r} \int_{(S)} \sigma \frac{\partial v_r}{\partial(\Delta S)} dS \qquad (1)$$

where $E' = E/(1-\nu^2)$, ν = Poisson's ratio, and ΔS is a virtual increment of the crack area. The derivative $\partial v/\partial(\Delta S)$ is called the weight function which of course depends on the specially chosen crack area increment ΔS. A procedure for the determination of the crack opening displacement field for a semi-elliptic surface crack was given by Fett and Munz (1997).
Two independent virtual crack changes that preserve the semi-elliptical crack shape were proposed by Cruse and Besuner (1975), namely, crack depth increment Δa with width c kept constant

$$\Delta S_A = \tfrac{1}{2}\pi c \Delta a \qquad (2)$$

or crack width increment Δc with depth a kept constant

$$\Delta S_B = \tfrac{1}{2}\pi a \Delta c \qquad (3)$$

as illustrated in Fig. 1b by the hatched areas.

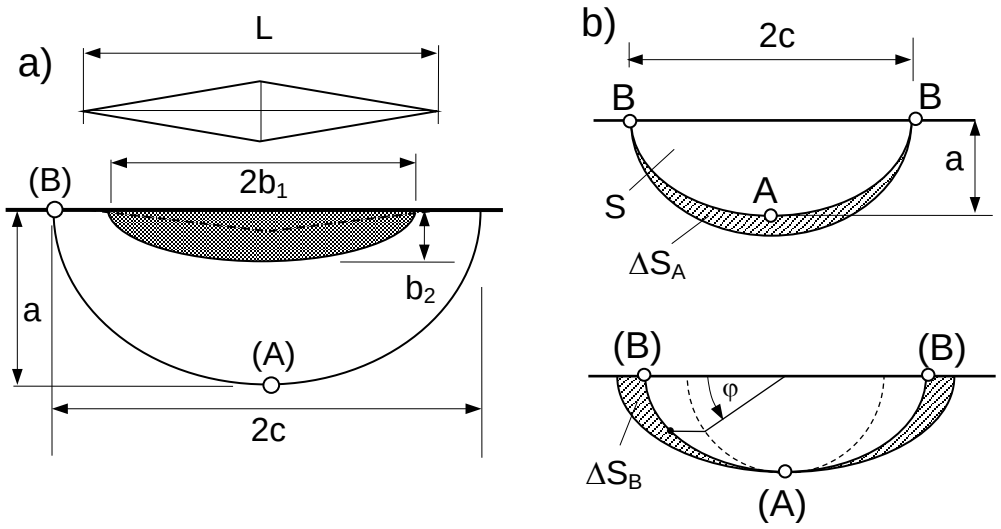

Fig. 1 a) Semi-elliptical crack (length 2*c*, depth *a*) loaded by a residual stress zone of length $2b_1$ and depth b_2, b) virtual crack extensions according to Cruse and Besuner (1975)

The stress intensity factors are represented by the geometric functions F_A (for a virtual crack increment at point A) and F_B (for an increment at the surface) according to

$$K_{A,B} = \sigma_0 \sqrt{\pi a} F_{A,B}, \qquad (4)$$

where σ_0 is a characteristic stress as the remote tensile stress or the outer fibre bending stress.

It should be emphasized that the Cruse-Besuner approach was examined intensively in the eighties and early nineties. Only a few papers may be mentioned in this context which show that the method is applicable to various types of cracks. The theoretical and experimental analyses on simple semi-elliptical surface cracks in plates and bars (see e.g. Görner et al. 1983, Caspers et al. 1990, Mahmoud 1990) were extended to more complicated crack problems as for instance almond- and sickle-shaped cracks in rods (Görner et al. 1983) and corner cracks (Varfolomeyev et al. 1991).

The use of this type of stress intensity factors allowed very good predictions for the development of the crack shape in tension and bending and correct predictions of crack growth rates in fatigue tests. In the following considerations only stress intensity factors defined by (1) will be addressed.

During loading of a Knoop indenter a residual stress zone develops below the contact area. According to the model proposed by Marshall (1983) a prolate spheroid was chosen for the shape of the irreversibly deformed 'plastic' zone with the ratio of the major axis b_1 and the depth b_2 (Fig. 1a). If σ_{res} is the residual stress assumed to be constant over the semi-elliptic cross section with the half-axes b_1 and b_2, the total force normal to the crack plane is

$$P_{res} = \tfrac{1}{2} \sigma_{res} \pi b_1 b_2 \qquad (5)$$

The stress intensity factors may be scaled with this force as

$$K_{A,B} = \frac{2P_{res}}{(\pi a)^{3/2}} F_{A,B} \qquad (6)$$

The geometric function $F_{A,B}$ in (6) are compiled in Fett (2009) in tables. For any parameter in the ranges of $1 \le c/b_1 \le \infty$, $1 \le b_1/b_2 \le \infty$, and $0.7 \le a/c \le 1.2$, F_B can be approximated by

$$F_B = -0.46 + 1.8\alpha + (0.55 + 0.531\alpha) \cdot \\ \cdot \exp[-(2.11 + 0.186\alpha)\sqrt{\frac{c}{b_1} - 0.97}] - \tfrac{1}{4}\left(\frac{b_1}{c}\right)^2 \left(\frac{1}{\beta} - \frac{1}{3}\right) \qquad (7)$$

with the abbreviations $\alpha = a/c$ and $\beta = b_1/b_2$.
For $1.1 \le c/b_1 \le \infty$, $1.5 \le b_1/b_2 \le \infty$, and $0.7 \le a/c \le 1$, F_A reads

$$F_A = 0.51 + 1.17\alpha - 0.645\alpha^2 - \\ -(1.317 + 6.18\alpha - 26.9/\beta^2) \exp[-3.7\sqrt{c/b_1}] \qquad (8)$$

Figure 2a represents the geometric function for the surface points (B) at $a/c = 0.85$ (see e.g. Marshall (1983) and Lube 2001) as a function of the ratios c/b_1 and b_1/b_2. The hatched area indicates the data region found from fracture surface observations on MgO-containing Si_3N_4 by Lube (2001). It can be concluded from Fig. 2a that the variation of F_B with ratio b_1/b_2 is less than 3% for $2 \le b_1/b_2 \le 6$.
For the limited parameter ranges of $0.7 \le a/c \le 1$, $1.2 \le c/b_1 \le 2$, and $2 \le b_1/b_2 \le 6$, the results in Fett (2009) can be approximated simply by

$$F_B \approx -0.742 + 1.869\frac{a}{c} + 0.69\frac{b_1}{c} - 0.0904\frac{b_2}{b_1} \qquad (9)$$

$$F_A \approx 1 + 0.022\left(\frac{a}{c}\right)^2 - 0.116\frac{b_1}{c} + 0.1717\frac{b_2}{b_1} \qquad (10)$$

Equations (5) and (6) consider residual forces P_{res} acting normal to the crack plane. In a Knoop indentation tests, the load P acting in indentation direction is given. Using the proportionality between P_{res} and P the stress intensity factor can be written as

$$K_{A,B} = \chi\left(\frac{E}{H}\right)^{1/2} \frac{P}{(\pi a)^{3/2}} F_{A,B} = \chi\left(\frac{E}{H}\right)^{1/2} \frac{P}{(\pi c)^{3/2}} \left(\frac{c}{a}\right)^{3/2} F_{A,B} \qquad (11)$$

adopting the ratio E/H according to Lawn et al. (1980) with an a priori unknown coefficient χ.

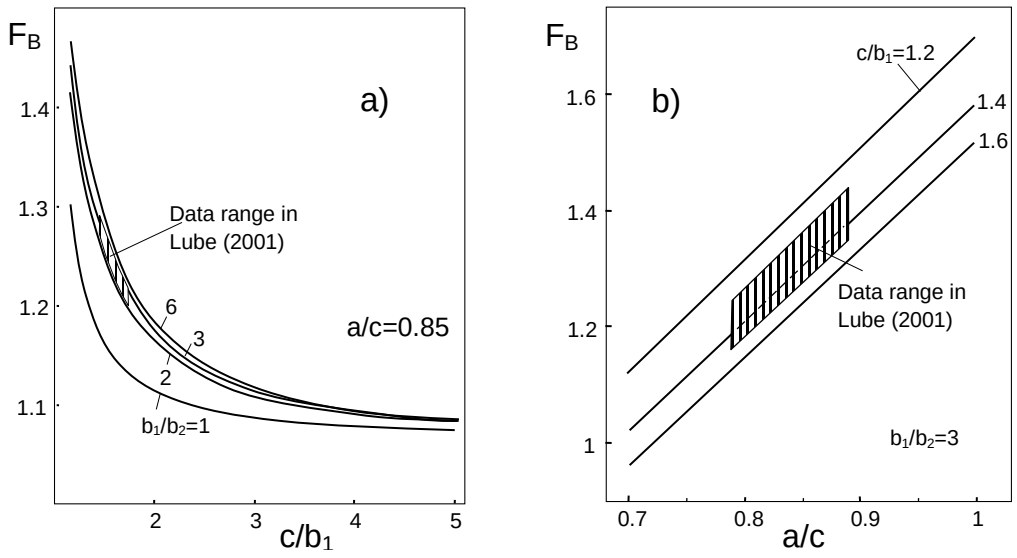

Fig. 2 Geometric function at point (B): a) for constant a/c=0.85, b) for constant b_1/b_2=3

3. Application to experimental results

Many experimental investigations on Knoop indentation cracks are known from literature. But only in a few cases all the parameters b_1, b_2, a/c and a (or c) are reported as required for the computation of the stress intensity factor. In a paper by Lube (2001) a gas-pressured silicon nitride containing 3% MgO (ESK, Kempten, Germany) was investigated from which all dimensions are available necessary for an evaluation of the stress intensity factor at the surface, K_B. This material showed an average Knoop-hardness of HK=12.2 GPa in the range of 50N≤P≤300N and a Young's modulus E=306 GPa.

Knoop indentations were made for a load range of 29 N≤P≤294 N and the dimensions of decorated cracks were measured on the crack face as well as by sectioning from the side normal to the crack plane. The resulting data are plotted in Fig. 3a. The axis ratio of the residual stress zone was determined as $b_1/b_2 \cong 2.9 \pm 0.5$. The length of the deformed zone was found to be somewhat smaller than the large indentation diagonal, namely, $2b_1 \approx 0.8L$. For the evaluation of the ordinate in Fig. 3b, the individual data from Fig. 3a were used. The solid symbols represent the stress intensity factor at the surface, K_B, the open squares the values at the deepest point, K_A, which are lower by roughly 20% (see also Keer et al. 1986). The increase of K_B with increasing crack length probably reflects the fact that the material exhibits an increasing R-curve for crack increments comparable with the length of the Knoop indentation cracks (cp. Fig. 4).

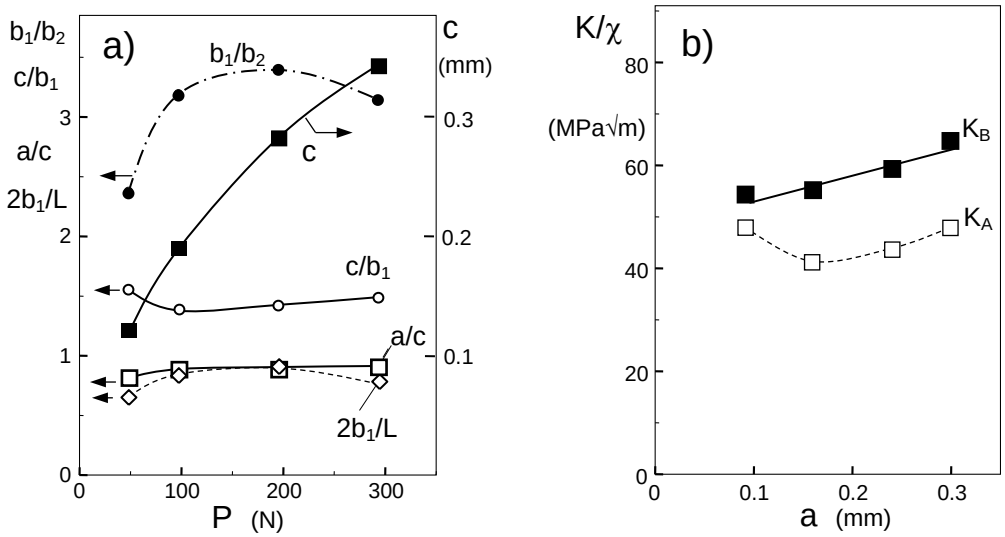

Fig. 3 a) Dimensions of crack and deformation zone for Knoop indentation cracks (Lube 2001) in MgO-containing Si_3N_4 versus indentation load, b) evaluation according to eqs. (7, 8, 11)

Under the assumption that the often present lateral crack system will not affect the stress intensity factor too strongly (see e.g. Cook and Pharr 1990), the residual stress intensity factor should match the fracture toughness. The unknown parameter χ may then be estimated by comparing the results of K_B in Fig. 3b with the K_R-curve for indentation cracks. Figure 4 shows the R-curve from measurements as decribed by Fünfschilling et al. (2010) on a bending bar with a deep notch of relative initial depth a_0/W=0.75 where W is the width of the bar. This curve is in good agreement with an R-curve in Lube (2004) constructed on the basis of pre-cracked bars. By application of the weight function procedure in Fett (2008) the R-curve for semi-circular indentation cracks was computed which is about 0.5MPa√m lower. There are several reasons for this lower K_R, which are based on the specific toughening mechanism that is relevant in the investigated material. In silicon nitrides toughening is achieved by crack face bridging by elongated grains (see e.g. Li et al. 1992). For an indentation crack, crack opening displacements near the indenter impression are larger than for a through crack of the same length which renders grain bridging at this location less effective. Another reason is the fact that for identical bridging stress relations the bridged area is smaller for indentation cracks than for through cracks due to the existence of the compressive zone without bridges. By taking the K_R of Fig. 4 for the same crack extensions (a, c in Fig. 3b and Δa in Fig. 4) as the values for K_B/χ we obtain

$$\chi \cong 0.10 \text{ to } 0.115 \qquad (12)$$

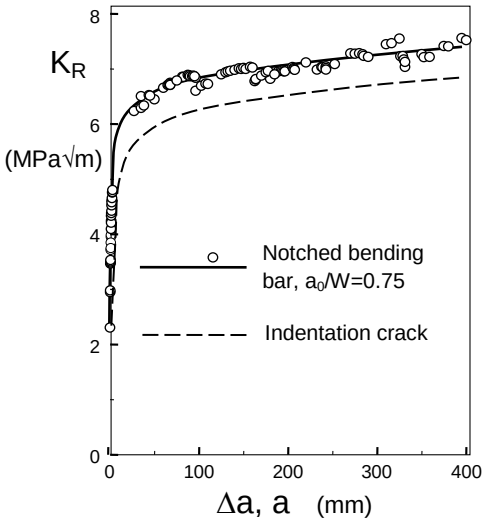

Fig. 4 R-curve for Ekasin-S (ESK, Kempten, Germany) estimated from tests on deeply notched bending bars; the R-curve for indentation cracks was computed by the method described by Fett et al. (2008), the abscissa for the indentation crack is given by *a*

Summary

During Knoop indentation tests the irreversibly deformed and damaged zone under the indenter causes residual stresses. These stresses give rise to a residual stress intensity factor and a resultant crack loading that reaches its peak value upon complete removal of the indentation load. The residual stress intensity factors at the surface and at the deepest point of the semi-elliptical crack were determined by the Cruse and Besuner weight function approach and expressed by simple relations valid over a large range of crack and residual stress zone geometries.
The solutions were applied to experiments on a gas-pressured silicon nitride ceramic.

The authors acknowledge D. B. Marshalls critical contribution to this manuscript.

References

Caspers M, Mattheck C, Munz D (1990) Propagation of surface cracks in notched and unnotched rods. ASTM STP 1060:365-389.
Cook RF, Pharr GM (1990) Direct Observation and Analysis of Indentation Cracking in Glasses and Ceramics. Journal of the American Ceramic Society 73:787-817.
Cruse TA, Besuner PM (1975) Residual life prediction for surface cracks in complex structural details. Journal of Aircraft 12:369-375.
Fett T, Munz D (1997) Stress intensity factors and weight functions. Computational Mechanics Publications, Southampton, UK.
Fett T, Fünfschilling S, Hoffmann MJ, Oberacker R (2008) Different R-curves for 2- and 3-dimensional cracks. International Journal of Fracture 153:153-159
Fett T (2009) Stress intensity factors, T-stresses, Weight function (Supplement Volume), IKM55. KIT Scientific, Publishing, Karlsruhe; (open Access: http://digbib.ubka.uni-karlsruhe.de/volltexte/1000013835).

Fünfschilling S, Fett T, Oberacker R, Hoffmann MJ, Özcoban H, Jelitto H, Schneider GA, Kruzic JJ (2010) R-curves from compliance and optical crack-length measurements. Journal of the American Ceramic Society 93:2814-21
Görner F, Mattheck C, Munz D (1983) Change in geometry of surface cracks during alternating tension and bending. Zeitschrift für Werkstofftechnik 14:11-18.
Keer LM, Farris TN, Lee JC (1986) Knoop and Vickers indentation in ceramics analyzed as a three-dimensional fracture. Journal of the American Ceramic Society 69:392-96.
Lawn BR, Evans AG, Marshall DB (1980) Elastic/plastic indentation damage in ceramics: The medial/radial crack system. Journal of the American Ceramic Society 63:574-81.
Li C-W, Lee D-J, Lui S-C (1992) R-Curve Behaviour and Strength for In-Situ Reinforced Silicon Nitrides with Different Microstructures. Journal of the American Ceramic Society 75:1777-85.
Lube, T (2001) Indentation crack profiles in silicon nitride. Journal of the European Ceramic Society 21:211-218.
Lube T, Fett T (2004) A threshold stress intensity factor at the onset of stable crack extension of Knoop indenttion cracks. Engineering Fracture Mechanics 71:2263-2269.
Mahmoud MA (1990) Surface fatigue crack growth under combined tension and bending loading. Engineering Fracture Mechanics 36:389-395.
Marshall DB (1983) Controlled flaws in ceramics: A comparison of Knoop and Vickers indentation. Journal of the American Ceramic Society 66:127-131.
Varfolomeyev IV, Vainshtok VA, Krasowsky AY (1991) Prediction of part-through crack growth under cyclic loading. Engineering Fracture Mechanics 40:1007-1022.